



Mandibular biomechanics of *Crocota crocuta*, *Canis lupus*, and the late Miocene *Dinocrocota gigantea* (Carnivora, Mammalia)

ZHIJIE JACK TSENG^{1,2*} and WENDY J. BINDER^{2,3}

¹Integrative and Evolutionary Biology Program, Department of Biological Sciences, University of Southern California, 3616 Trousdale Parkway, Los Angeles, California 90089, USA

²Natural History Museum of Los Angeles County, 900 Exposition Boulevard, Los Angeles, California 90007, USA

³Biology Department, Loyola Marymount University, 1 LMU Drive, Los Angeles, California 90045, USA

Received 3 July 2008; accepted for publication 10 December 2008

The relative simplicity of the mandible and its functional integration with the upper dentition in carnivorans makes it an ideal subject for functional morphological studies. To compare the mandibular biomechanics of two convergently evolved bone-cracking ecomorphologies, we used finite element modelling to analyse mandibular corpus stress. The bone-cracking spotted hyena *Crocota crocuta* was used as a living analogue to the late Miocene percrocotid *Dinocrocota gigantea*, using the grey wolf *Canis lupus* as a molar bone-crushing outgroup. Mandibular stress values during p3, p4, and m1 tooth biting are found to be lowest in *Cr. crocuta*, and elevated in both *Ca. lupus* and *D. gigantea*. However, the stress-dissipation patterns of the pre-m1 corpus are similar between *Cr. crocuta* and *D. gigantea*. Lastly, *D. gigantea* has a relatively weaker corpus at the post-m1 position than either *Cr. crocuta* or *Ca. lupus*. These findings suggest that even though stress patterns are similar amongst the bone-cracking ecomorphs, the extinct *D. gigantea* had a weaker mandibular structure when performing a comparable bone-cracking task as in *Cr. crocuta* because of its slender post-m1 corpus. Ontogeny could potentially play an important role in strengthening the post-m1 corpus by growth in the dorsoventral axis, and continuous increase in biting performance through adulthood in living *Cr. crocuta* suggests the possibility of a relatively more delayed development to full bone-cracking capability in *D. gigantea*.

© 2009 The Linnean Society of London, *Zoological Journal of the Linnean Society*, 2010, 158, 683–696.
doi: 10.1111/j.1096-3642.2009.00555.x

ADDITIONAL KEYWORDS: bone cracking – bite strength – finite element modelling.

INTRODUCTION

Families and species of the mammal order Carnivora show diverse ecological adaptations from herbivory to hypercarnivory (Werdelin, 1996), and this dietary diversity is reflected in the specialization of craniodental morphology (Van Valkenburgh, 1988, 1989). Large carnivores have been categorized into guilds by their ecomorphologies, with a range of killing strategies, and these include groups such as bone crackers, meat specialists, etc. (Biknevicius & Van Valkenburgh, 1996). Perhaps the most well-known and

studied extant bone-cracking specialist is the spotted hyena *Crocota crocuta*, which is a dominant social predator in sub-Saharan Africa, and an adept hunter which also has the ability to crack and consume bones of small and large prey (Kruuk, 1972).

Common to many bone-cracking specialists, *Cr. crocuta* is characterized by a robust cranium and hypertrophied dentition, in addition to high dorsoventral bending strength in its mandibular corpus (Biknevicius & Ruff, 1992). For a given mandibular length, the mandibular corpus of *Cr. crocuta* is especially robust ventral and caudal to the precarnassial bone-cracking premolars, which may serve to resist forces produced in processing particularly hard food

*Corresponding author. E-mail: jack.tseng@usc.edu

items such as bone. These traits appear to be functional aspects of the bone-cracking ecomorphology.

In the fossil record, the major ecomorphologies within the carnivoran guild have been continuously occupied throughout the Cenozoic (meat specialists, bone specialists, omnivores, etc.), albeit by taxa with disparate phylogenetic affinity (Werdelin, 1989; Van Valkenburgh, 1991). The bone-cracking ecomorphology is found in different phylogenetic groups, and this is particularly amenable to study as durophagous carnivores are easily identified through their craniodental morphology, which includes a robust skull and highly domed frontal regions in the cranium, along with hypertrophied dentition adapted for processing hard food (Werdelin, 1989; Stefen & Rensberger, 2002). Two large lineages that have evolved these bone-cracking ecomorphologies include the borophagine canids (Wang, Tedford & Taylor, 1999) and the Hyaenidae (Werdelin & Solounias, 1991). A third group, more closely related to the hyaenid lineage, is a family of feliform carnivorans of very large size with exceptional craniodental robustness (Qiu, Xie & Yan, 1988). The largest species in this group, *Dinocrocuta gigantea*, remains enigmatic for the lack of a complete postcranial skeleton to reveal its locomotory mode and thus its ecological niche.

As an example of specialization, the biomechanics of the skull of durophagous carnivores are of particular interest as they demonstrate the resistance of the skull to extreme food types, and can reveal constraints of what extant animals can consume as well as indicators of the limits and adaptations of extinct carnivores. Studies of feeding adaptation using mandibles have several advantages over those using crania. The mandible is critical in producing and also resisting forces incurred during feeding, and unlike the cranium is a single bone that is not under simultaneous selective constraints for sensory functions and protection of the brain, etc. Furthermore, the mandible is a relatively strong skeletal element that is better preserved and represented in the carnivoran fossil record than complete crania, allowing a more complete understanding of macroevolutionary patterns of morphological and functional change. Previous studies of jaw geometry, mechanical advantage of jaw musculature, and bone stress and strain using mandibular models have provided both experimental and theoretical foundations for further inquiry into the masticatory biomechanics of mandibles (Greaves, 1982, 1985; Hylander, 1985, 1986; Dechow & Hylander, 2000; Ross *et al.*, 2007).

For these reasons, we used the mandible as the element of comparison between the living *Cr. crocuta* and the extinct *D. gigantea* bone-cracking ecomorphs. The purpose of this study was to better understand the bone-cracking carnivoran ecomorphology exemplified by the living spotted hyena, and compare it with

an extinct durophagous carnivore which evolved in a different lineage during the late Miocene epoch of Asia (~11–10 Mya). We evaluate the biomechanical similarities amongst morphologically identified bone crackers by examining the ability of the mandibular corpus at the tooththrow to resist and distribute stress incurred during several biting scenarios.

To this purpose, we utilize a comparative finite element modelling approach to analyse the relative stress and strain magnitudes and distributions in the mandibular corpus of the two carnivorans. As demonstrated by Binder & Van Valkenburgh (2000), the bite force of *Cr. crocuta* continues to increase through adult life, and is an indication of persistent musculoskeletal growth and/or remodelling. The only suitable specimen of the fossil percrocutid *D. gigantea* we could locate for this study represents that of a subadult individual, judging from its partially erupted upper canines, lack of tooth wear on the cheek teeth, unfused cranial sutures, and relatively small size compared to an ontogenetic series of fossil skulls from contemporaneous sedimentary deposits in Gansu Province, China. For the bone-cracking comparison, we decided to use a subadult *Cr. crocuta* skull that also showed the above features of an immature individual.

The extant grey wolf, *Canis lupus*, was used as a control representing a nonbone-cracking meat specialist. Although *Ca. lupus* does consume bones, as defined by Werdelin (1989), it is a bone crusher, as it crushes bones with the first and/or second set of molars, rather than the premolars. In fact, as *Ca. lupus* is hypothesized to be an ecological equivalent of some basal bone-cracking hyaenids (Werdelin & Solounias, 1996; Turner, Antón & Werdelin, 2008), this species is a particularly apt outgroup. We chose to compare an adult *Ca. lupus* with subadult *Cr. crocuta* and *D. gigantea* because it makes for a particularly conservative comparison as we know that it will not underestimate the jaw strength and stresses of *Ca. lupus* in comparison with the larger species.

Finite element modelling is an engineering method used to approximate solutions of real world complex physical problems, and has been developed and used in mechanical engineering for decades. More recently, this method has begun to be used effectively in understanding the functional adaptations and limitations of vertebrates. The application of this technique to analyse 3D structures in vertebrates was recently reviewed by Rayfield (2007). For analysis of vertebrate skulls, in particular, earlier work on theropod dinosaurs using 2D finite element modelling (Rayfield, 2005) has provided an initial example of the utility of this method in comparative functional morphology. Subsequent work by McHenry *et al.* (2006) on the theoretical rostrum morphology of various crocodylian forms has also broadened the horizon of

the application to discover potential evolutionary pathways and more generalized adaptive patterns. More recently, work on the mammalian frontal sinus by Farke (2008) and Tanner *et al.* (2008) has demonstrated uses of computer-modified morphologies in detecting adaptive signals in current morphological structures. Others examining modern and recently fossilized skulls have used multiple (heterogeneous) material properties and *in vivo* muscle data to approximate actual stresses and strains (McHenry *et al.*, 2007; Moreno *et al.*, 2008). Using a comparative approach of original morphologies with technique developed in Dumont, Piccirillo & Grosse (2005) and Grosse *et al.* (2007), we test a specific hypothesis regarding the adaptiveness of the robust mandibular morphology of three living and extinct carnivoran taxa: the bone-cracking ecomorphs *Cr. crocuta* and *D. gigantea* have robust mandibular corpuses that resist dorsoventral bending stress incurred during bone-cracking bites with the premolars, and thus would have lower stress than molar bone-crushing *Ca. lupus*, which does not consume large bones with the anterior premolars.

INSTITUTIONAL ABBREVIATIONS

IVPP, Institute of Vertebrate Paleontology and Paleoanthropology, Beijing, China; LACM(Mamm), mammalogy collection of the Natural History Museum of Los Angeles County, Los Angeles, California, USA.

METHODS

The methodology utilized in this study was similar to that outlined in detail by Tseng (2009). A shorter summary of the model-building protocol is included here in the main text, but interested readers are referred to the Appendix for a more technically detailed description. One mandible from each species was used, so that interpretation of the analytical results could be restricted to the comparison of sagittal bending in the dentate mandibular corpus of the comparative taxa.

Skulls of a *Cr. crocuta* [LACM(Mamm) 30655], *Ca. lupus* [LACM(Mamm) 23010], and *D. gigantea* (IVPP V15649) were scanned with computer tomography (CT) at the University of California, Los Angeles Medical Center (Fig. 1). The *D. gigantea* specimen is the most complete known for this species; however, the unworn dentition and unfused cranial frontal and parietal sutures indicate that it is a subadult individual. Therefore, a subadult individual of *Cr. crocuta* was chosen to make the two bone-cracking ecomorphs more comparable in terms of ontogenetic age. A fully adult *Ca. lupus* skull was chosen to represent a large individual with full capability for hypercarnivory as a

nonbone-cracking control (for definition of bone cracking see Introduction). CT data were imported into the Mimics medical imaging software (Materialise N.V., Leuven, Belgium) and a digital reconstruction was created. The reconstruction was then smoothed and checked for errors and artefacts of digitization in the rapid prototyping software GEOMAGIC STUDIO 10 (Geomagic, Inc., Research Triangle Park, North Carolina, USA). The reconstruction was then built into a 3D element mesh in the finite element modelling and analysis software STRAND7 (G + D Computer Pty Ltd, Sydney, Australia), where model parameters were assigned. The most important anatomical parameters were the attachment sites of the temporalis, masseter, and internal pterygoid muscles, which were given their relative forces with lines of action directed at sites of origination in the cranium.

Muscle insertion sites were identified on the three models with comparison to a dissection carried out on a *Hyaena hyaena* skull [LACM(Mamm) 97200]. The masticatory muscles were removed from the skull by carefully dissecting the fibres along the base of the cranial origination sites and mandibular insertion sites. The attachment regions of the temporalis, masseter, and internal pterygoid muscles were reproduced using modelling clay on a plastic cast of the *D. gigantea* mandible to visually aid the delineation of those sites on the computer models (Fig. 2). In addition, the relative force contributions of the modelled muscles were assigned based on the relative mass of those muscles extracted from the dissection specimen. The estimated mass of the temporalis muscle was 190 g, extrapolated by the remaining temporalis muscle on the dissection specimen (76 g, ~40% of total) after a veterinary necropsy removed the parietal region of the cranium to extract the brain. The masseter muscle complex (superficial and deep) had a mass of 65 g; the internal pterygoid had a mass of 18 g. A muscle contribution ratio of 69.6% temporalis to 23.8% masseter to 6.6% internal pterygoid was used in all three models. These ratios are close to those reported by Turnbull (1970) from a *Ca. lupus* dissection (68.2% temporalis to 24.2% masseter to 7.6% pterygoid). Relative muscle masses were used as a proxy for the relative force production capability of the masticatory muscles; other studies have utilized physiological cross-sectional areas (PCSA) of the jaw muscles to estimate input force (Ross *et al.*, 2005), but as such data are lacking for carnivorans, we chose not to use PCSA to estimate muscle forces. The implications of this assumption in our models are discussed below in the context of the results.

Validation studies combining finite element models and *in vivo* strain data for macaques have shown that the bones of the cranium are best modelled as elastically orthotropic elastic material when using homo-

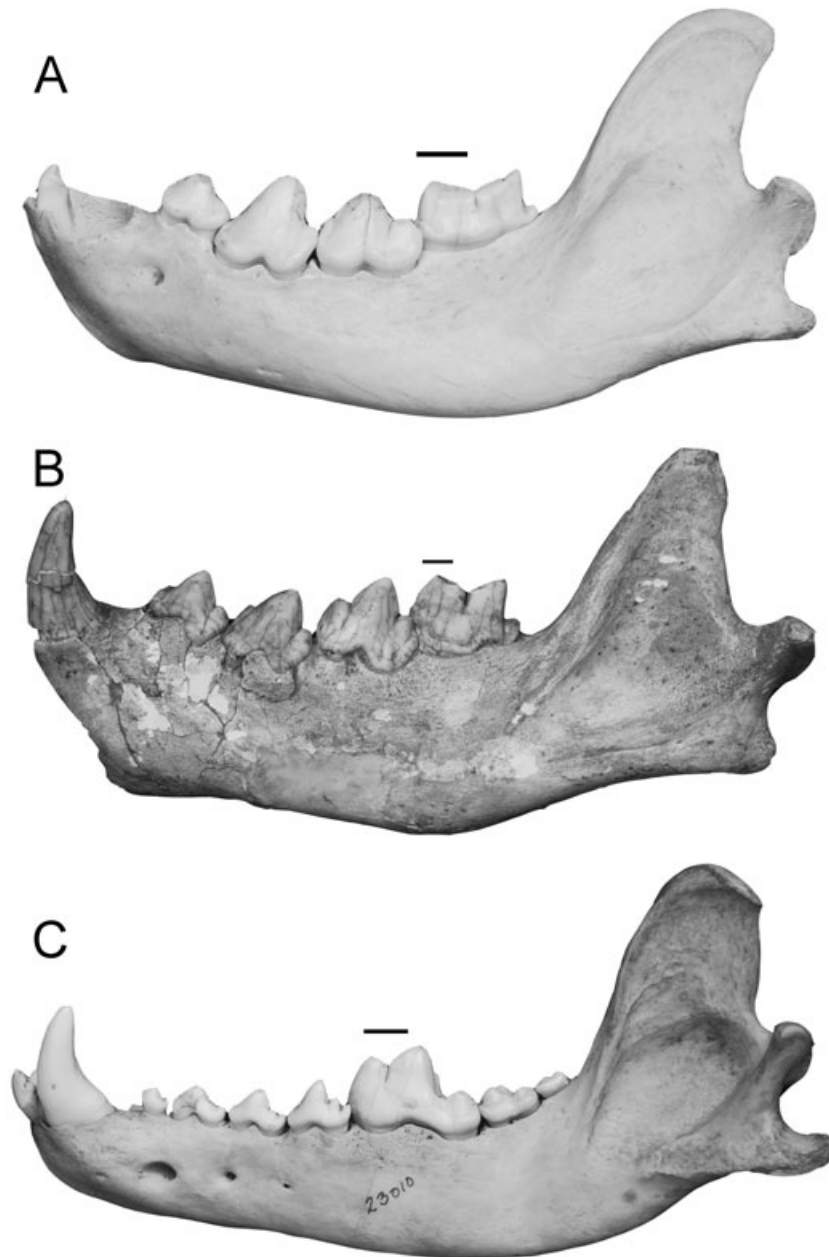


Figure 1. Photos of specimens used in the study. A, *Crocuta crocuta* [LACM(Mamm) 30655], left mandible; B, *Dinocrocuta gigantea* (IVPP V15649), right mandible; C, *Canis lupus* [LACM(Mamm) 23010], left mandible. Specimens are scaled to approximately the same length in figure. Scale bars [over carnassial tooth (m1)] = 10 mm.

geneous material properties (Strait *et al.*, 2005). As we restrict our study to the cortical region of a single mandibular bone, we used material properties of an elastic isotropic material to represent the mandible models; there is some previous evidence as to the validity of this approach (Ashman *et al.*, 1985). A Young's modulus of 20 GPa and a Poisson's ratio of 0.3 were used in all the models; these values are typical of mammalian cortical bone (Erickson, Cat-

anese & Keaveny, 2002) and represent a compromise between the more pliable bone and more brittle enamel, which were modelled as the same material. Because we are interested in the relative mechanical behaviour of the mandibles and not the exact response at boundaries of different materials, multiple material properties were not utilized. Thus structures such as the connective tissues between teeth and bone, and the cancellous bones were not

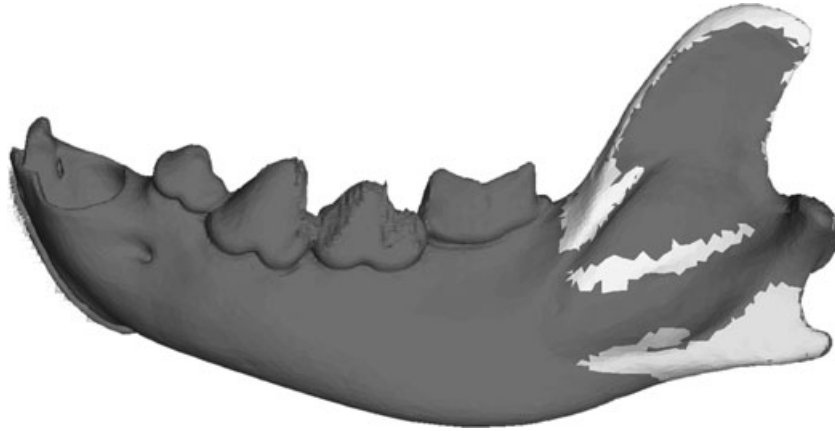


Figure 2. Muscle attachment sites on the mandible finite element models, with *Crocuta crocuta* as an example. The light areas on top of the ascending ramus and in the mandibular fossa are attachment sites for the temporalis. The light area on the angular process is the attachment site of the masseter. The internal pterygoid attachment (not shown) is on the medial side of the angular process.

included. One added advantage of this simplified approach is to allow direct comparison between extant and fossil jaws, as diagenesis prohibits direct observation of density differences in the teeth and jaws, the densities being proxies for assigning material properties in our methodology.

Three sets of analyses were conducted. In all analyses the models of *Ca. lupus* and *D. gigantea* were standardized to the length of *Cr. crocuta* (Fig. 1). By standardizing length, the analytical results can be interpreted in the context of functional differences by partially removing body size influence (Biknevičius & Ruff, 1992). The models were constrained from movement at the mandibular symphysis, bite position, and the temporomandibular joint to simulate a bone-cracking bite causing dorsoventral bending. The analysis simulates an instantaneous event at static equilibrium, and for the purposes of examining overall patterns of stress distribution in the corpus we did not include mobility at the temporomandibular joint or mandibular symphysis. Under these assumptions, we exclude the potential effects of torsion during unilateral biting when balancing and working side muscles are differentially activated, and instead examined mainly dorsoventral bending forces. In the first analysis, the extant taxa *Cr. crocuta* and *Ca. lupus*, with models of their original morphology, were loaded with the same muscle force of 5891.63 N. This input force is required to produce the maximum bite force at the lower carnassial tooth (m1) of a 12-month-old (the estimated age of the skull used) *Cr. crocuta* calculated from the regression equation given by Binder & Van Valkenburgh (2000). Biting at the p3, p4, and m1 was tested. The results of the analyses are summarized using Von Mises stress and strain

values, which are combined measures of how close a material is to failure. The stress and strain values were standardized by first multiplying the element values by their element volumes, then dividing by the median element volume of each model. Median is used because it is a robust measure of central tendency in nonparametric distributions such as the distribution of stress and strain values (Zar, 1999). Typical finite element models produce analytical results with a large number of low-stress elements and a small number of high-stress elements, and thus are poorly characterized by parametric summary statistics. Results for the second and third analyses are presented in this way as well.

In the second analysis, models of all three taxa were modified so that the medullary cavities of the corpses were removed. This was carried out to compare directly the fossil *D. gigantea* mandible, for which the mandibular medullary cavity could not be distinguished, with the extant specimens. This set of analyses also allowed the comparison between the original and solid models of *Cr. crocuta* and *Ca. lupus*, providing an estimate of how much the results of the solid *D. gigantea* might deviate from an analysis of the original morphology, if it was preserved. All other parameters and input forces were held constant as in the first analysis. In the third analysis, the three solid models were modified so that a uniform bite force of 1000 N was produced at each of the three biting positions (p3, p4, m1, respectively). This allowed the examination of the relative efficiencies of the mandibles at distributing and resisting stress when an identical bite force is produced. Based on these experimental parameters, a total of 18 test cases was analysed.

RESULTS

ANALYSIS 1

For *Cr. crocuta*, the difference in median stress was much smaller between any two biting scenarios than in the same comparisons in *Ca. lupus*, and this is reflected in the stress distribution as well (Fig. 3). Median stress ranged from 5.58 MPa for m1 biting to 7.01 MPa for p3 biting (Table 1). Median strain followed a similar increase with 0.00036 for m1 biting to 0.00045 for p3 biting (Table 1). For *Ca. lupus* p3 and p4 biting produced similar magnitudes of stress and strain throughout the mandible, and m1 biting produced lower overall values (Table 1). The same patterns held true for values of median absolute deviation from median (MAD) for both stress and strain of the two models. The dispersion of stress values around the median (interquartile range, IQR) of the *Cr. crocuta* model is roughly 50% of the corresponding values for *Ca. lupus* (Table 1). For overall strain, the IQRs for *Cr. crocuta* are less than half the values of *Ca. lupus* in all biting scenarios. For the same amount of muscle input force, *Ca. lupus* produced higher bite forces than *Cr. crocuta* at all three biting positions. Bite force increased sequentially from p3 to m1 in *Ca. lupus*; in *Cr. crocuta* bite force was highest in m1 but lowest at p4 (Table 1).

ANALYSIS 2

Stress magnitudes increased slightly for all biting scenarios when an identical set of analyses were conducted on solid *Cr. crocuta* and *Ca. lupus* models (Table 2). Bite forces at p3 and p4 increased significantly in the solid *Cr. crocuta* model (145 and 245%, respectively), but m1 bite force only increased slightly (8.5%). For *Ca. lupus*, elevation in bite force in the solid model increased in magnitude across the board from p3 to m1 (16, 25, and 64%, respectively). Bite forces at p3 and p4 in *D. gigantea* were lower than either *Cr. crocuta* or *Ca. lupus*; the m1 bite force of *D. gigantea* was intermediate between *Cr. crocuta* and *Ca. lupus*. The percentage changes in stress from the original models to the filled models were of increasing magnitude from the p3 to the m1 position for *Ca. lupus* (5, 9, and 13% for the three bite scenarios, respectively). In *Cr. crocuta*, the increase in stress was smallest at the p4 position (7%), which also exhibited the largest increase in bite force; p3 experienced a 17% increase and m1 a 14% increase in median stress.

ANALYSIS 3

At 1000 N of p3 bite force, the mandible of *Cr. crocuta* had the lowest stress and *D. gigantea* the highest. The same pattern is true for 1000 N of p4 bite force, but for the m1 bite *Ca. lupus* had slightly lower stress than *Cr.*

crocuta. For both *D. gigantea* and *Ca. lupus* mandibular stress decreased from a p3 bite to a m1 bite, but for *Cr. crocuta* a p4 bite produced lower stress than in both p3 and m1 bites. MAD was substantially higher (by a factor of > 4) in *D. gigantea* and *Ca. lupus* than in *Cr. crocuta* for p3 and p4 biting, but for m1 *Ca. lupus* had the lowest MAD. *Dinocrocuta gigantea* and *Ca. lupus* shared similarly elevated levels of IQR compared to *Cr. crocuta*, but for m1 biting *Cr. crocuta* had a higher IQR than the other two taxa (Table 3).

The visualization of stress in the mandible models showed that high stress in *D. gigantea* and *Ca. lupus* is most concentrated in the anterior-facing slope of the coronoid process (Fig. 4E, F). The most anterior part of the mandible receives relatively little strain; visible increase in mandibular corpus strain is seen posterior of the p3 bite point in *Cr. crocuta*, immediately under the bite point in *D. gigantea*, and both anterior and posterior of the bite point in *Ca. lupus* (Fig. 4D–F). In *Cr. crocuta* most of the strain is concentrated ventral of the articular process on the buccal side; the lingual has more widespread but also more even strain around the angular process (Fig. 4A, D). In *D. gigantea* the entire mandibular corpus ventral and posterior of the p3 bite point has elevated strain; the highest strained regions are in the dorsal and ventral regions of the articular process and the anterior coronoid process (Fig. 4E). On the lingual side, high strain continues around both the anterior and posterior slope of the coronoid process, and connects on the lingual face of the ascending ramus (Fig. 4B). Regions of lower strain tapers off anterior of the m1, but the corpus below m1 still experiences elevated strain. Regions of elevated strain in *Ca. lupus* extend both anterior and posterior of the corpus below the p3 bite point (Fig. 4F); the corpus immediate below m1 has low strain. Posterior to this point, the strains are high on the anterior face of the coronoid process, and ventral of the articular process; the ascending ramus also shows higher strain than in the other two models (Fig. 4D–F). On the lingual side, strain is elevated near the mandibular symphysis, and gradually increases posterior of m1; the strain is even and widespread posterior to this point, except for high strain in the centre of the coronoid process and near the angular process (Fig. 4C). In the mandibular corpus beneath the cheek teeth *Cr. crocuta* has low and confined stress, whereas *Ca. lupus* and *D. gigantea* have more widespread stress distribution in the region. The most stressed regions in all three models were around the base of the ascending ramus.

For all three models, the median stress and strain experienced in the entire mandible was comparable between p3 and p4 biting, and lower for m1 biting (Fig. 5). This decrease in m1 biting is slight in *Cr. crocuta*, but more dramatic in *Ca. lupus* and *D. gigantea*.

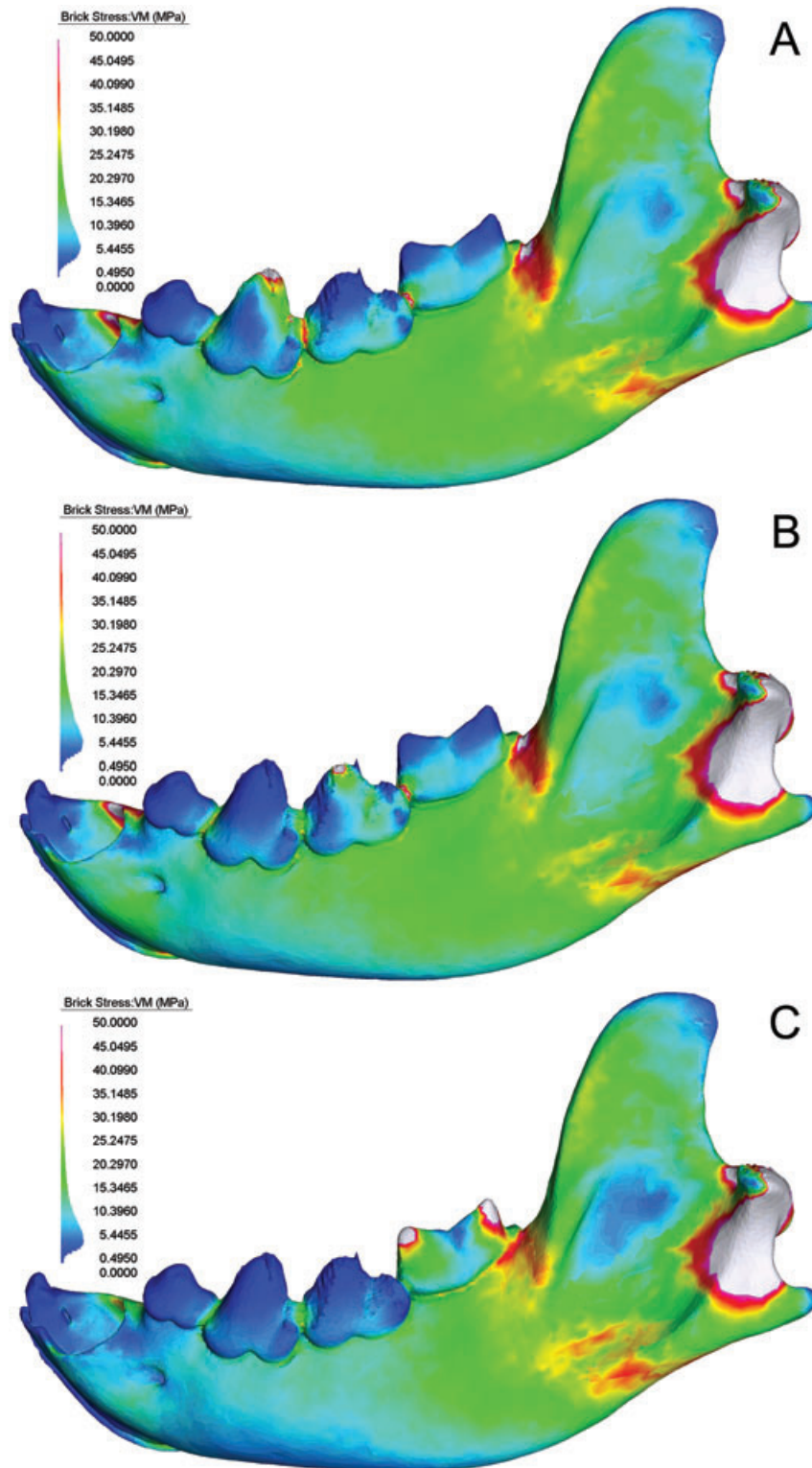


Figure 3. Stress distributions in the mandible of *Crocuta crocuta* in A, p3; B, p4, and C, m1 biting scenarios. Colour spectrum represents stress magnitude, with blue as low stress and white relatively high stress.

Table 1. Von Mises stress and strain values and bite forces from unmodified finite element models of *Crocota crocuta* and *Canis lupus* with uniform muscle force input of 5891.63 N

		Stress			Strain			Bite force
		Median	MAD	IQR	Median	MAD	IQR	
<i>Cr. crocuta</i>	p3	7.01	6.04	30.36	0.00045	0.00039	0.00197	334.6
	p4	6.69	5.77	29.6	0.00043	0.00038	0.00192	287.47
	m1	5.58	4.87	25.56	0.00036	0.00032	0.00166	468.12
<i>Ca. lupus</i>	p3	23.68	20.29	70.23	0.00154	0.00133	0.00457	563.31
	p4	22.41	19.32	66.55	0.00146	0.00127	0.00433	725.83
	m1	16.38	14.98	53.85	0.00105	0.00099	0.00351	906.63

Stresses are in MPa, strain in $\mu\epsilon$, and bite force is in Newtons.
MAD, median absolute deviation from median; IQR, interquartile range.

Table 2. Von Mises stress values for the solid finite element models of *Crocota crocuta*, *Dinocrocota gigantea*, and *Canis lupus* with an uniform muscle force input of 5891.63 N

		Median	MAD	IQR	Bite force	% + Median	% + MAD	% + IQR	% + Bite
<i>Cr. crocuta</i>	p3	8.49	7.55	30.18	822.26	0.17	0.20	-0.01	0.59
	p4	7.18	6.44	27.20	991.87	0.07	0.10	-0.09	0.71
	m1	6.51	5.96	27.32	472.10	0.14	0.18	0.06	0.01
<i>D. gigantea</i>	p3	22.96	20.49	61.21	528.06	-	-	-	-
	p4	22.35	19.84	57.69	663.16	-	-	-	-
	m1	17.11	15.54	44.69	975.45	-	-	-	-
<i>Ca. lupus</i>	p3	25.04	23.61	85.50	653.70	0.05	0.14	0.18	0.14
	p4	24.50	22.98	80.71	910.69	0.09	0.16	0.18	0.20
	m1	18.84	18.24	70.79	1484.09	0.13	0.18	0.24	0.39

Per cent changes of values compared to the original models are listed for the extant taxa. Median, MAD, and IQR of the stresses are in MPa; bite force is in Newtons.

MAD, median absolute deviation from median; IQR, interquartile range.

All interdental regions examined for *Cr. crocuta* (p3–p4, p4–m1, and post-m1) showed relatively little strain compared to the other two models (Fig. 6). A small strand of elevated strain is visible in the post-m1 cross-section on the dorsal–buccal part of the jaw (Fig. 6A). In *D. gigantea*, the entire buccal side of the p3–p4 and p4–m1 cross-sections shows elevated strain; the post-m1 cross-section has the highest strain at the dorsal–buccal edge, with the strain lower and spreading around both the dorsal and ventral edge onto the lingual side of the mandible (Fig. 6B). In *Ca. lupus*, the entire buccal side and the ventral–lingual side of the p3–p4 cross-section show elevated strain; at the p4–m1 cross-section the strain is only slightly elevated, and is concentrated in the ventral–buccal region (Fig. 6C). In the m1–m2 cross-section, the entire ventral side and both ventral–lingual and ventral–buccal sides of the mandibular corpus have higher strain.

Table 3. Von Mises stress values for the filled and scaled finite element models of *Crocota crocuta*, *Dinocrocota gigantea*, and *Canis lupus*

		Median	MAD	IQR
<i>Cr. crocuta</i>	p3	10.32	9.19	36.71
	p4	7.24	6.49	27.42
	m1	13.80	12.63	57.87
<i>D. gigantea</i>	p3	46.70	41.75	123.85
	p4	35.60	31.75	92.20
	m1	19.04	17.26	49.54
<i>Ca. lupus</i>	p3	38.82	36.61	132.00
	p4	25.19	23.63	82.71
	m1	12.86	12.45	48.45

All models were analysed with a bite force of 1000 N at the respective bite positions.

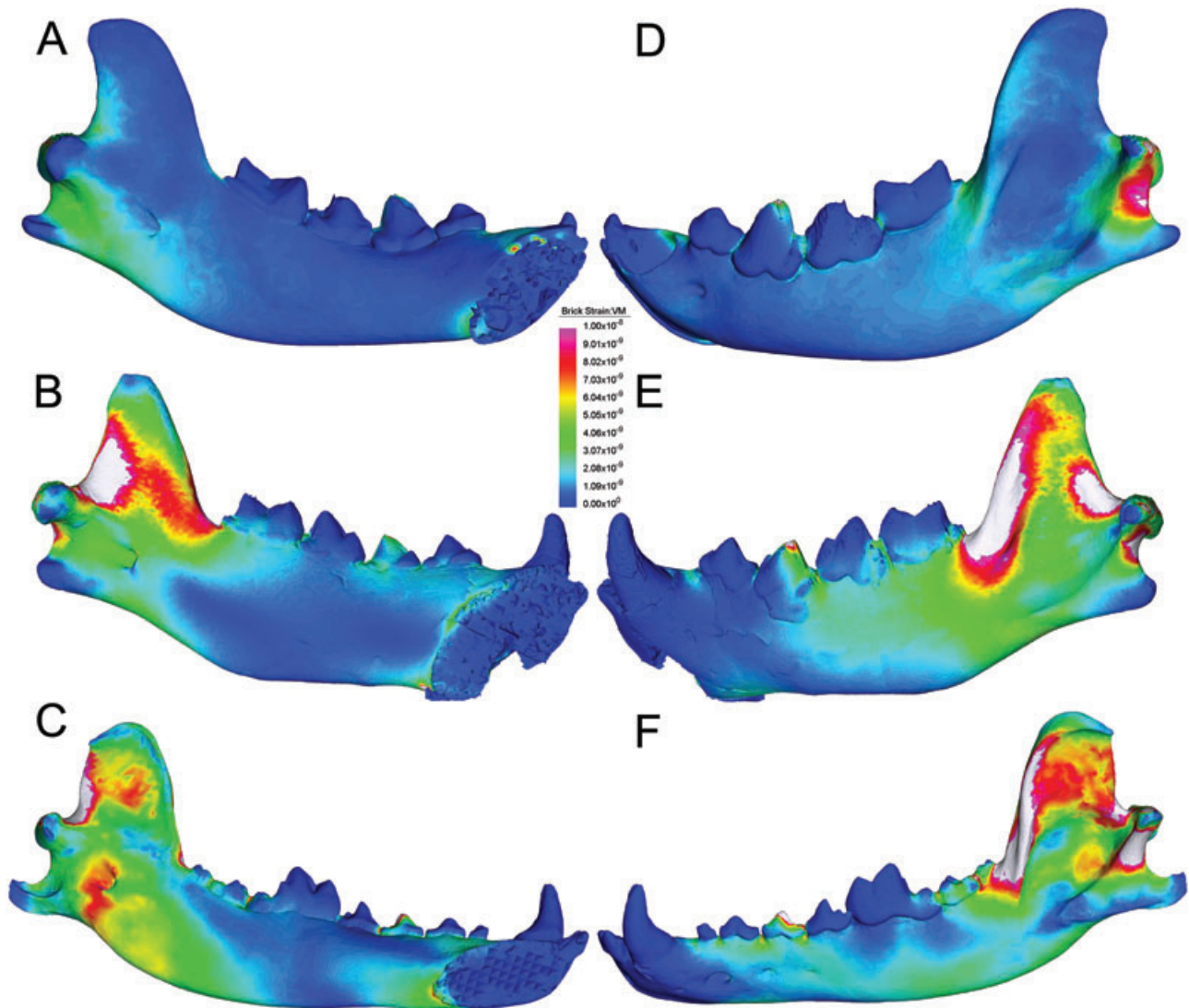


Figure 4. Comparison of strain distributions during a p3 biting scenario in *Crocuta crocuta* (A, lingual; D, buccal), *Dinocrocuta gigantea* (B, lingual; E, buccal), and *Canis lupus* (C, lingual; F, buccal).

Overall, the stress and strain values decrease gradually from p3, p4, to m1 biting for *Cr. crocuta*; they are comparable between p3 and p4 biting in *Ca. lupus* and *D. gigantea*, and lower for m1 biting. The distribution of stress and strain values is less variable in *Cr. crocuta* than in *D. gigantea*; both are less variable than *Ca. lupus*. In cross section, the mandibular corpus stress is minimal in *Cr. crocuta*; in *D. gigantea* it is concentrated on the buccal wall, and in *Ca. lupus* it is spread around the buccal, ventral, and lingual walls.

DISCUSSION

Whereas the mammalian cranium is under simultaneous selective pressure on its sensory and mechanical functions, the mandibles are simpler in that their

main function is mastication. This makes the mandible a good system for studying evolutionary questions regarding dietary adaptations because of its 'single-purpose' function and morphological simplicity in being a single unit of bone. Consistent with previous findings of strong correlation between mandibular corpus strength and dietary adaptation (Biknevicius & Ruff, 1992; Therrien, 2005), the profile of median strain across different biting scenarios are more consistent in *Cr. crocuta* than in *Ca. lupus* (Fig. 5). *Crocuta crocuta*, a habitual bone-cracking predator, demonstrates adaptations for using the p3, p4, or m1 positions equally well in its mandibular corpus structure. *Canis lupus*, however, experiences visibly lower stress and strain in m1 biting than for p3 or p4 biting (Fig. 5). This is likely to be associated with the use of

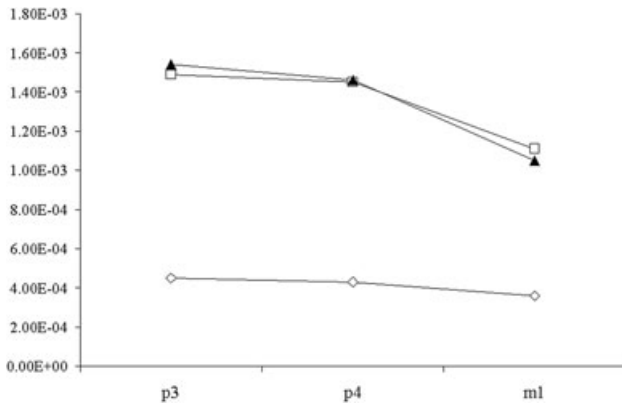


Figure 5. Median strain values at different bite positions for *Crocota crocuta* (open diamond), *Canis lupus* (filled triangle), and *Dinocrocuta gigantea* (open square).

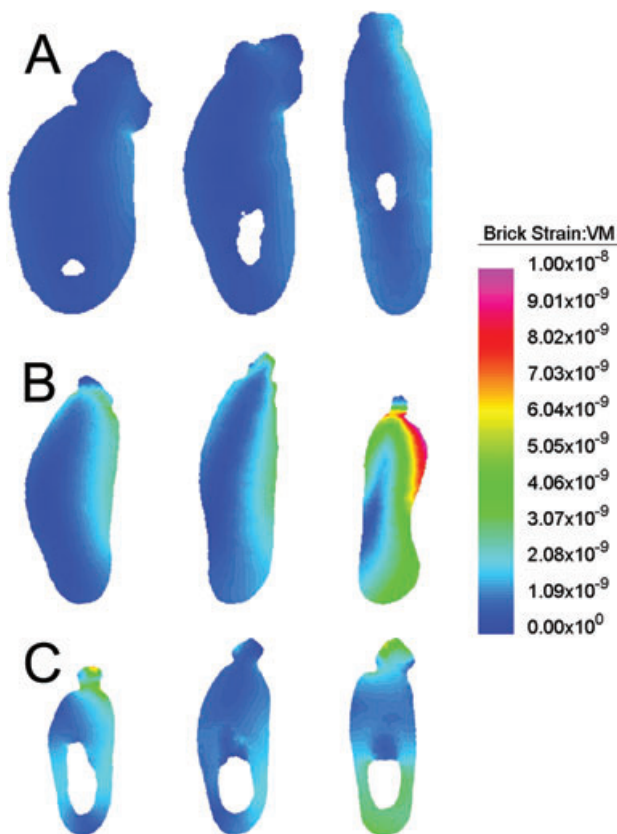


Figure 6. Cross-section strain profiles for (from left to right): p3–p4, p4–m1, and post-m1 interdental spaces in A, *Crocota crocuta*, B, *Dinocrocuta gigantea*, and C, *Canis lupus* during a p3 bite. View is from rostral towards caudal; buccal is to the right.

premolar tooth use to crack bone in *Cr. crocuta*, and the concentration on m1 function for shearing meat in *Ca. lupus*. The position of the lower carnassial in *Cr. crocuta* is more posteriorly situated in the dentary

than the same tooth in *Ca. lupus* (Biknevicius & Ruff, 1992; Biknevicius, 1996); this is further indication of functional differences in the tooth position for greatest force production in the two species. Complementing previous data on inferred functional differences in the biting behaviour of the two species from dental morphology and mandibular structure, our results are consistent with the known differences in *Cr. crocuta* and *Ca. lupus*, the former using premolars to crack bone, whereas the latter uses postcarnassial molars (including the talonid basin of m1) in processing hard foods.

The cross-section images of the *Cr. crocuta* and *Ca. lupus* mandible models further demonstrate the correspondence between corpus strength and predator ecology. The interdental cross-sections at p3–p4, p4–m1, and post-m1 of the *Cr. crocuta* jaw all show relatively little strain during p3 biting (Fig. 6A). Along with only minor changes in overall strain when changing bite positions, the mechanical behaviour of the mandible (i.e. high strength throughout the length of the corpus) is consistent with how this species uses both the anterior premolars for bone cracking and the carnassial (m1) for meat consumption. *Canis lupus*, however, has the lowest strain during m1 biting (Fig. 5). This shows the emphasis of this hypercarnivore on the shearing component of the dentition, as can be seen from the low stress in the entire region ventral of the carnassial even during p3 biting (Fig. 4C). Surprisingly, in this context, the mandible of *D. gigantea* is similar to *Ca. lupus* in that there is lowered stress and strain incurred during m1 biting, but it is similar to *Cr. crocuta* in terms of similar strain distributions in the p3–p4 and p4–m1 regions during p3 biting, as would be expected for a bone-cracking species (Fig. 6B). The weakest region of the *D. gigantea* mandible is in the post-m1 regions, where the corpus is most likely not yet fully developed in this individual. Although it has been noted in the past that *D. gigantea* may be a bone cracker, this analysis functionally demonstrates a similarity between the biomechanics of *Cr. crocuta* and *D. gigantea*, giving further evidence that jaw morphology does indeed demonstrate functionality. The lack of postcarnassial molars in both may demonstrate a common result of the evolution of the premolars as the bone-cracking teeth in these groups. Another interesting line of investigation in functional convergence would be to examine the cranial and mandibular biomechanics of the North American borophagine canids, which would have used a combination of the upper carnassial and the lower p4 and carnassial for bone cracking (Werdelin, 1989; Wang *et al.*, 1999).

Overall, the mandible of *Cr. crocuta* experiences much lower stress and strain values than in both *D.*

gigantea and *Ca. lupus* (Fig. 4; Tables 1, 2). Given the same length, *Cr. crocuta* is much better at resisting bending than the other two species. This is unexpected because the cranium of *D. gigantea* has previously been shown to be just as 'well-designed' for a simulated bone-cracking bite as the spotted hyena (Tseng, 2009). Even though Tseng (2009) used bone volume to standardize the cranium models whereas this study uses standardized length, a series of checks run with volume-standardized mandible models return similar results as to the ones shown for length-standardization (not presented here). A recent study comparing the implications between different scaling methods suggests that model surface area standardization allows stress and strain energy to be directly compared given identical loading forces (G. Slater, pers. comm.); we obtained similar results using surface area standardization compared to those presented here, the major difference being smaller differences in median stress and strain amongst the three models.

Our interpretation of the results does not change when comparing the original morphology models to the fossil *D. gigantea*, or with models where the medullary cavity is filled (Tables 1, 2). This provides a degree of robustness to our results. Given the same mandible, however, bite force increases in the filled models from the original models. This is taken to represent the more efficient conduction of forces through a more homogeneous bone medium in the filled mandibles (Table 3). Given these results, it is interesting to note that the medullary cavities of *Cr. crocuta* and *D. gigantea* (where visible) appear to be relatively smaller compared to *Ca. lupus* during our examination of the CT images. The reduced medullary cavity in the bone-cracking carnivores might thus be a modification to increase cortical volume within the mandibular corpus and more efficient force transmission during biting.

As mentioned in the Introduction and Methods, given the nearly fully erupted permanent dentition and presence of sutures in the frontal and parietal bones, the *D. gigantea* specimen used in this study was most likely a subadult, and the *Cr. crocuta* specimen was chosen to roughly match the developmental stage of the *D. gigantea* specimen studied. Nevertheless, the manner in which development occurs may not be the same in these species. The difference in stress and strain in the mandibles of these two specimens could represent differential ontogenetic paths of bone growth. Whereas the mandibular corpus appears relatively deep and robust in *Cr. crocuta*, the *D. gigantea* mandibular corpus has a relatively underdeveloped post-m1 region when compared to several adult specimens in a late Miocene fossil fauna in northern China (Z. J. Tseng, pers. observ.). This gives support to a relative developmental delay in dorsoventral deepening

of the posterior mandibular corpus in the larger *D. gigantea* when compared with *Cr. crocuta*.

To summarize, our results do not unambiguously support our hypothesis that the bone-cracking taxa share similar stress distributions and low stress levels in the mandibular corpus during a simulated bone-cracking bite. Even though *Cr. crocuta* and *D. gigantea* exhibit similar stress distribution patterns, the stress levels in *D. gigantea* are more similar to *Ca. lupus* in all biting scenarios tested. This result may be explained by ontogenetic differences in tooth use and mandibular shape in *D. gigantea*, and/or a different masticatory strategy compared to *Cr. crocuta*.

IMPLICATIONS

Even though the results presented in this study show clear differences amongst taxa representing different ecomorphologies, ontogeny appears to be an important factor that requires further examination. For extant carnivores, this would require analysis of an ontogenetic series of mandibles using finite element modelling to reveal differences in stress and strain distribution in the mandibular corpus through development. A better understanding of the biomechanical changes in the masticatory apparatus of these carnivores around the weaning period would be especially useful for estimating the life history of juvenile carnivores in the fossil record. For example, if *D. gigantea* juvenile individuals indeed had a relatively delayed development of the posterior mandibular corpus compared to *Cr. crocuta*, it could imply either a prolonged weaning period (similar to and perhaps extending beyond that of *Cr. crocuta*), and/or a switch in prey preference from smaller to larger species or individuals if *D. gigantea* was similar to *Cr. crocuta* in its bone-cracking behaviour. The critical transitional period between a mixed deciduous-permanent dentition to fully permanent dentition in *Cr. crocuta* occurs around the time of weaning (Biknevicius, 1996); it leaves room for speculation as to whether *D. gigantea* had a similar constraint through ontogeny with the development of its mandibular corpus. In addition, the social structure of each carnivore species could affect the growth phases of the mandibular corpus, which might be involved in agonistic interactions amongst conspecifics (Biknevicius & Leigh, 1997). This information becomes particularly useful if the timing and duration of deciduous and permanent dental eruption in fossil taxa can be incorporated (e.g. Feranec, 2004) to estimate absolute durations of juvenile dental development. There is evidence that there are further morphological changes and performance changes such as increasing bite force, which can occur even after the complete eruption of adult teeth and body size (Binder & Van Valkenburgh, 2000; Benoit,

2006). Although these are difficult to detect using standard morphological measurements, finite element analysis may be sensitive enough to detect patterns that are associated with these types of functional changes. Thus, better understanding of *Cr. crocuta* jaw development may give greater insight into the understanding of fossil species such as *D. gigantea*.

The analyses conducted in this study are linearly static, with full constraint of the temporomandibular joints and the mandibular symphysis. A fruitful future direction would be to incorporate some degree of mobility at the joints, and use a dynamic analysis to examine additional dissipation or concentration of stress across these joints (Greaves, 1988). Furthermore, the stress distribution at different gapes can also be studied in a dynamic analysis to reveal potential optima in gape angle and inferred prey bone size. In conjunction with the addition of these modified constraints, the left and right mandibles should be analysed together to include the asymmetric effects of a unilateral bite on the stress and strain of balancing versus working side corpus (Greaves, 1983). Lastly, the addition of heterogeneous material properties at least to the enamel of the dentition would provide a more realistic model.

The comparison of our dissection muscle mass proportions to published estimates for *Cr. crocuta* has some implications for bite force estimates in extinct taxa. The assignment of muscle proportions from the *H. hyaena* dissection to the model of *Ca. lupus* was a good approximation of the muscle mass proportions for *Ca. lupus* in Turnbull (1970), which listed ratios of temporalis 68.2% to masseter 24.2% to pterygoid 7.6% (5 : 3.2 : 1). As a check, all three models were also analysed with these proportions, and the resulting stress and strain were indistinguishable from those obtained using dissection proportions. Both empirical values are dramatically different from the muscle cross-sectional areas estimated by the dry skull method (Thomason, 1991; Wroe, McHenry & Thomason, 2005), which gave proportions of temporalis 55.92% to masseter 44.08 (1.3 : 1) for *Cr. crocuta*. Given potential differences in muscle densities, which might affect assignment of relative muscle forces as estimated by muscle mass and cross-section area, one might expect these percentages not to match. However, the published bite force estimate for *Cr. crocuta* using the dry skull method (Wroe *et al.*, 2005) is lower than forces measured *in vivo* (Binder & Van Valkenburgh, 2000) by up to 100%. Specifically, the contribution of the temporalis muscle is higher from a dry skull estimate, and the masseter smaller. As the temporalis has a longer in-lever arm than the masseter, its underestimation tends to have a larger effect on underestimating bite force, and thus may partially explain this difference in muscle force estimates.

CONCLUSION

Finite element models of *Cr. crocuta*, *Ca. lupus*, and *D. gigantea* were constructed and used in a comparative biomechanical analysis of stress and strain in the mandibular corpus. Results suggest that for a given mandibular length, *Cr. crocuta* experiences much lower stress and strain than *Ca. lupus* or *D. gigantea*. The lower stress and strain in *Cr. crocuta* is also more consistent across different biting scenarios, indicating a mandibular corpus more generally adapted for unpredictable loads. *Canis lupus* and *D. gigantea*, however, showed lowest stress and strain when biting with the m1 carnassial. However, the stress and strain distributions in *D. gigantea* during p3 and p4 biting are more equivalent to *Cr. crocuta* than *Ca. lupus*, suggesting that mandibular corpus of *D. gigantea* is in part similarly adapted to *Cr. crocuta*. The slight increase in mandibular stress in filled corpus models from models with medullary cavities, coupled with more significant increases in bite force, indicates that the thick cortical bone mass of the bone-cracking taxa provides more efficient force transmission. Further examination of ontogenetic series of *Ca. lupus* and *Cr. crocuta* could reveal life history differences that reflect the divergent ecomorphologies represented in adult individuals, and serve as a comparative basis for life history studies in extinct carnivoran taxa.

ACKNOWLEDGEMENTS

We thank X. Wang (LACM) for helpful discussions on the structure of the study; Z. Qiu (IVPP) for a loan of *D. gigantea*; J. Dines (LACM) for access to *Ca. lupus* and *Cr. crocuta*; M. McNitt-Gray (UCLA) for scanning the specimen; B. Dumont (UMass Amherst) provided the BONELOAD program for modelling muscle forces; software purchase was supported by a USC Zumberge interdisciplinary grant and a grant-in-aid from the American Society of Mammalogists; research was supported by a NSF graduate research fellowship (Z. J. T.).

REFERENCES

- Ashman RB, Rosinia G, Cowin SC, Fontenot MG. 1985. The bone tissue of the canine mandible is elastically isotropic. *Journal of Biomechanics* **18**: 717–721.
- Benoit M. 2006. Multiphasic allometric analysis in lions (*Panthera leo*): life history expressed through morphometrics. *Journal of Vertebrate Paleontology* **26**: S41A.
- Biknevicius AR. 1996. Functional discrimination in the masticatory apparatus of juvenile and adult cougars (*Puma concolor*) and spotted hyenas (*Crocuta crocuta*). *Canadian Journal of Zoology* **74**: 1934–1942.

- Biknevicius AR, Leigh SR. 1997.** Patterns of growth of the mandibular corpus in spotted hyenas (*Crocuta crocuta*) and cougars (*Puma concolor*). *Zoological Journal of the Linnean Society* **120**: 139–161.
- Biknevicius AR, Ruff CB. 1992.** The structure of the mandibular corpus and its relationship to feeding behaviors in extant carnivores. *Journal of Zoology* **228**: 479–507.
- Biknevicius AR, Van Valkenburgh B. 1996.** Design for killing: craniodental adaptations of predators. *Carnivore Behavior, Ecology, and Evolution* **2**: 393–428.
- Binder WJ, Van Valkenburgh B. 2000.** Development of bite strength and feeding behaviour in juvenile spotted hyenas (*Crocuta crocuta*). *Journal of Zoology* **252**: 273–283.
- Dechow PC, Hylander WL. 2000.** Elastic properties and masticatory bone stress in the macaque mandible. *American Journal of Physical Anthropology* **112**: 553–574.
- Dumont ER, Piccirillo J, Grosse IR. 2005.** Finite-element analysis of biting behavior and bone stress in the facial skeletons of bats. *The Anatomical Record Part A* **283A**: 319–330.
- Erickson GM, Catanese J III, Keaveny TM. 2002.** Evolution of the biomechanical material properties of the femur. *The Anatomical Record* **268**: 115–124.
- Farke AA. 2008.** Frontal sinuses and head-butting in goats: a finite element analysis. *The Journal of Experimental Biology* **211**: 3085–3094.
- Feranec RS. 2004.** Isotopic evidence of saber-tooth development, growth rate, and diet from the adult canine of *Smilodon fatalis* from Rancho La Brea. *Palaeogeography, Palaeoclimatology, Palaeoecology* **206**: 303–310.
- Greaves WS. 1982.** A mechanical limitation on the position of the jaw muscles of mammals the one-third rule. *Journal of Mammalogy* **63**: 261–266.
- Greaves WS. 1983.** A functional analysis of carnassial biting. *Biological Journal of the Linnean Society* **20**: 353–364.
- Greaves WS. 1985.** The generalized carnivore jaw. *Zoological Journal of the Linnean Society* **85**: 267–274.
- Greaves WS. 1988.** A Functional consequence of an ossified mandibular symphysis. *American Journal of Physical Anthropology* **77**: 53–56.
- Grosse I, Dumont ER, Coletta C, Tolleson A. 2007.** Techniques for modeling muscle-induced forces in finite element models of skeletal structures. *The Anatomical Record* **290**: 1069–1088.
- Hylander WL. 1985.** Mandibular function and biomechanical stress and scaling. *American Zoologist* **25**: 315–330.
- Hylander WL. 1986.** *In-vivo* bone strain as an indicator of masticatory bite force in *Macaca fascicularis*. *Archives of Oral Biology* **31**: 149–157.
- Kruuk H. 1972.** *The spotted hyena: a study of predation and social behavior*. Chicago: The University of Chicago Press.
- McHenry C, Clausen PD, Daniel WJT, Meers MB, Pendharkar A. 2006.** Biomechanics of the rostrum in crocodylians, a comparative analysis using finite element modeling. *The Anatomical Record Part A* **288A**: 827–849.
- McHenry C, Wroe S, Clausen PD, Moreno K, Cunningham E. 2007.** Supermodeled sabercat, predatory behavior in *Smilodon fatalis* revealed by high-resolution 3D computer simulation. *Proceedings of the National Academy of Sciences of the United States of America* **104**: 16010–16015.
- Moreno K, Wroe S, Clausen PD, McHenry C, D'Amore DC, Rayfield EJ, Cunningham E. 2008.** Cranial performance in the Komodo dragon (*Varanus komodoensis*) as revealed by high-resolution 3-D finite element analysis. *Journal of Anatomy* **212**: 736–746.
- Qiu Z-X, Xie J-Y, Yan D-F. 1988.** Discovery of the skull of *Dinocrocota gigantea*. *Vertebrata Palasiatica* **26**: 128–138.
- Rayfield EJ. 2005.** Aspects of comparative cranial mechanics in the theropod dinosaurs *Coelophysis*, *Allosaurus*, and *Tyrannosaurus*. *Zoological Journal of the Linnean Society* **144**: 309–316.
- Rayfield EJ. 2007.** Finite element analysis and understanding the biomechanics and evolution of living and fossil organisms. *Annual Review of Earth and Planetary Science* **35**: 541–576.
- Ross CF, Dharia R, Herring SW, Hylander WL, Liu Z-J, Rafferty KL, Ravosa MJ, Williams SH. 2007.** Modulation of mandibular loading and bite force in mammals during mastication. *Journal of Experimental Biology* **210**: 1046–1063.
- Ross CF, Patel BA, Slice DE, Strait DS, Dechow PC, Richmond BG, Spencer MA. 2005.** Modeling masticatory muscle force in finite element analysis: sensitivity analysis using principal coordinates analysis. *The Anatomical Record Part A* **283A**: 288–299.
- Stefen C, Rensberger JM. 2002.** The specialized enamel structure of hyaenids (Mammalia, Hyaenidae): description and development within the lineage – including percrocotids. *Zoologische Abhandlungen* **52**: 127–147.
- Strait DS, Wang Q, Dechow PC, Ross CF, Richmond BG, Spencer MA, Patel BA. 2005.** Modeling elastic properties in finite-element analysis: how much precision is needed to produce an accurate model? *The Anatomical Record Part A* **283A**: 275–287.
- Tanner JB, Dumont ER, Sakai ST, Lundrigan BL, Holkamp KE. 2008.** Of arcs and vaults: the biomechanics of bone-cracking in spotted hyenas (*Crocuta crocuta*). *Biological Journal of the Linnean Society* **95**: 246–255.
- Therrien F. 2005.** Mandibular force profiles of extant carnivores and implications for the feeding behaviour of extinct predators. *Journal of Zoology* **267**: 249–270.
- Thomason JJ. 1991.** Cranial strength in relation to estimate biting forces in some mammals. *Canadian Journal of Zoology* **69**: 2326–2333.
- Tseng ZJ. 2009.** Cranial function in a late Miocene *Dinocrocota gigantea* (Mammalia: Carnivora) revealed by comparative finite element analysis. *Biological Journal of the Linnean Society* **96**: 51–67.
- Turnbull WD. 1970.** Mammalian masticatory apparatus. *Fieldiana: Geology* **18**: 149–356.
- Turner A, Antón M, Werdelin L. 2008.** Taxonomy and evolutionary patterns in the fossil Hyaenidae of Europe. *Geobios* **41**: 677–687.
- Van Valkenburgh B. 1988.** Trophic diversity in past and present guilds of large predatory mammals. *Paleobiology* **14**: 155–173.

- Van Valkenburgh B. 1989.** Carnivore dental adaptations and diet: a study of trophic diversity within guilds. In: Gittleman JL, ed. *Carnivore behavior, ecology, and evolution*. Vol. I. New York: Cornell University Press, 410–436.
- Van Valkenburgh B. 1991.** Iterative evolution of hypercarnivory in canids (Mammalia: Carnivora): evolutionary interactions among sympatric predators. *Paleobiology* **17**: 340–362.
- Wang X, Tedford RH, Taylor BE. 1999.** Phylogenetic systematics of the Borophaginae (Carnivora: Canidae). *Bulletin of the American Museum of Natural History* **243**: 1–391.
- Werdelin L. 1989.** Constraint and adaptation in the bone-cracking canid *Osteoborus* (Mammalia: Canidae). *Paleobiology* **15**: 387–401.
- Werdelin L. 1996.** Carnivoran ecomorphology: a phylogenetic perspective. In: Gittleman JL, ed. *Carnivore behavior, ecology, and evolution*. Vol. II. New York: Cornell University Press, 582–624.
- Werdelin L, Solounias N. 1991.** The Hyaenidae: taxonomy, systematics and evolution. *Fossils and Strata* **30**: 1–104.
- Werdelin L, Solounias N. 1996.** The evolutionary history of hyaenas in Europe and western Asia during the Miocene. In: Bernor RL, Rietschel S, Mittmann W, eds. *The evolution of Western Eurasian Miocene mammal faunas*. New York: Columbia University Press, 290–306.
- Wroe S, McHenry C, Thomason JJ. 2005.** Bite club: comparative bite force in big biting mammals and the prediction of predatory behaviour in fossil taxa. *Proceedings of the Royal Society of London. Series B. Biological Sciences* **272**: 619–625.
- Zar JH. 1999.** *Biostatistical analysis*. Upper Saddle River: Prentice-Hall.

APPENDIX

FINITE ELEMENT MODELLING PROTOCOL

1. Reconstruction from computer tomography (CT) data: the skulls were scanned with a Siemens Definition 64 scanner (Siemens Medical Solutions, Forchheim, Germany) at 0.6 mm slice thickness and interslice distance. This produced 464 images for *Crocota crocuta*, 499 for *Canis lupus*, and 616 for *Dinocrocota gigantea*. The images were exported in the DICOM file format into MIMICS. Within MIMICS, the cranium and mandibles were segmented separately, but a correct articulation position was maintained. For *D. gigantea*, the mandibular cavity was filled with sediment in which the fossil was preserved. No attempts were made to remove the sediments because of difficulty in distinguishing bone from sediment. The segmented masks were simplified using MIMICS' remeshing function, and the resulting 3D reconstruction exported as stereolithography (*.stl) files.
2. Reconstruction improvement and smoothing: the stereolithography files were then imported into GEOMAGIC STUDIO. The mandibular surface reconstructions were first decimated in triangle count and then refined to represent 50 000 total triangles in *Cr. crocuta* and *Ca. lupus*, and 100 000 triangles in *D. gigantea*. The 'sandpaper' and 'fill holes' functions were used to remove sharp surface features that are artefacts from segmentation and surface mesh generation. The reconstructions were checked for intersecting triangles, and when no errors were found, the reconstructions were exported as separate cranium and mandibles stereolithography files for each specimen.
3. Finite element model: the stereolithography files were then imported into STRAND7, and first cleaned by removing duplicate nodes that represent junctions of triangle corners created in the ASCII stl format (as opposed to binary). The surface reconstructions were then checked for errors in free triangle edges and t-junctions. If an error was found, the reconstruction was modified in GEOMAGIC STUDIO and then re-imported into STRAND7. Once the surface reconstructions were error-free, they were solid-meshed with four-noded tetrahedral elements. The *Cr. crocuta* model had 48 3033 (original morphology) and 12 5892 (filled corpus) elements. The *D. gigantea* mandible model had 118 8858 elements, and the *Canis lupus* model had 429482 (original morphology) and 130693 (filled corpus) elements. The cranium associated with each set of mandibles was then imported into STRAND7. The forces calculated for each muscle were saved as a text file, which was imported into the BONELOAD program (Grosse *et al.*, 2007), where force vectors simulating muscles wrapping around the bone surface were created over the entire surface of each muscle attachment sites. The material properties of $E = 20$ GPa (Young's modulus) and $\rho = 0.3$ (Poisson's ratio) were assigned, and the mandibular symphysis, bite position, and the temporomandibular joint were fixed from any movement. A linear static analysis was then run with each scenario. Calculation time per scenario was approximately 20 min for *Cr. crocuta* and *Ca. lupus*, and 40 min for *D. gigantea* because of the higher degrees of freedom created by the larger number of tetrahedral elements.